

# Effect of current density on the composition of Zn-Ni alloy deposits and the characteristics of the trivalent chromium passive film on these deposits

Le Ba Thang<sup>1</sup>, Truong Thi Nam<sup>1,\*</sup>, Le Duc Bao<sup>1</sup>, Nguyen Thi Thanh Huong<sup>1</sup>,  
Uong Van Vy<sup>1</sup>, Le Thao Ly<sup>2</sup>

<sup>1</sup>*Institute of Materials Science, Vietnam Academy of Science and Technology*

*18 Hoang Quoc Viet, Nghia Do, Ha Noi, Viet Nam*

<sup>2</sup>*VNU University of Science, Vietnam National University, Hanoi*

*334 Nguyen Trai, Thanh Xuan, Ha Noi, Viet Nam*

\*Email: [namtruong1208@gmail.com](mailto:namtruong1208@gmail.com)

Received: 10 October 2023 ; Accepted for publication: 13 October 2025

**Abstract.** The aim of this research is to investigate the influence of the composition of zinc-nickel (Zn-Ni) alloy coatings on the color and properties of chromium (III) passive films, with a specific focus on their corrosion protection abilities. The composition, phase structure, and morphology of these coatings were analyzed using energy dispersive spectrometry, X-ray diffractometry, and scanning electron microscopy, respectively. Additionally, chronopotentiometry and potentiostatic methods were employed to analyze the possible causes of the composition and structure changes induced by deposition current density. The results showed that the zinc-nickel alloy of interest has a body centered cubic (bcc) lattice structure and has a chemical formula of Ni<sub>5</sub>Zn<sub>21</sub>. The Ni content of Zn-Ni coatings is about 12÷15 %. Efficiency at current density of 1 A/dm<sup>2</sup> is the highest at 94.1 %, efficiency at current density of 5 A/dm<sup>2</sup> is the smallest at 74.67 %, plating particles with dimensions in the range of 0.01 ÷ 1µm. All of TCP films on the Zn-Ni alloys deposited at different current densities meet DIN EN ISO 19598: 2017-04 standards.

**Keywords:** Zn-Ni alloy deposits, chromium(III) passivation film, corrosion protection

**Classification numbers:** 2.5.3

## 1. INTRODUCTION

Zinc (Zn) coatings have been widely used for protecting materials, especially steel, from corrosion. However, the protective capabilities of pure zinc coatings are still quite limited. Zinc has been studied in combination with other metals such as nickel, iron, and cadmium to become zinc alloys. Among them zinc-nickel (Zn-Ni) alloys with varying nickel content have found numerous successful applications in enhancing the protection of surface materials [1 - 4].

Zn-Ni coatings are widely applied due to several advantages. They offer better corrosion resistance for steel compared to pure zinc and zinc-cadmium alloy coatings. Additionally, they

exhibit increased hardness [4] and improved thermal stability, outperforming several other alloy coatings [2 - 4].

The properties of Zn-Ni alloy coatings depend on various factors, including the composition and pH of the plating galvanizing bath, temperature [3], current density, electrode potential, and the application mode of the coating (pulse or DC). Nickel plays a crucial role in reducing the electrochemical corrosion resistance of the Zn-Ni alloy coating by inhibiting the hydration of  $\text{Zn(OH)}_2$  into the corrosion product (ZnO). Hydroxides have lower electrical conductivity than oxides, leading to weaker cathodic oxygen reduction and thus a lower corrosion rate. The alloy's composition is significantly influenced by the ratio of  $[\text{Zn(II)}]/[\text{Ni(II)}]$  in the galvanizing bath. Zn-Ni coatings with 10 - 15 % nickel by weight exhibit improved corrosion resistance, ductility, and good weldability. Besides chemical composition, the physical properties of Zn-Ni coatings depend on microstructure, phase chemistry, and structural parameters. Notably, the corrosion resistance of Zn-Ni is significantly better than that of other zinc coatings. Furthermore, increasing the nickel content in the coating up to 12-15% by weight further improves corrosion resistance. Beyond 15 % wt% nickel content, corrosion resistance decreases [1, 2].

To enhance the corrosion resistance of zinc-nickel alloy coatings, various passive solutions containing Cr(III) ions, such as molybdate, vanadate, titanate, and silica have been extensively researched [1,5,6]. These solutions have gained acceptance in the automotive industry worldwide. Passive layers containing  $\text{Cr}^{3+}$  ions offer several advantages, including non-toxicity and corrosion resistance equivalent to traditional  $\text{Cr}^{6+}$ -containing passive layers. Research on the morphology, structure, and chemical composition of these passive layers highlights the significant role of chromate passivation in corrosion protection, a topic of interest for many researchers [1, 5 - 8].

## 2. EXPERIMENTALS

### 2.1. Sample preparation

Low carbon steel plates ( $40 \times 50 \times 1$  mm) were degreased by immersion in the solution of 60 g/L UDYPREP-110EC (Enthone) at 50 - 60 °C for 5-10 min. After that the samples were immersed into solution containing HCl (10 %V) and urotropine (3.5 g/L) at ambient temperature for 2 - 5 min.

Zn-Ni alloy deposits were obtained by electrodeposition from the solutions shown in Table 1. The plating times were 12, 15, 20, 30, and 60 min. Current densities were 1, 2, 3, 4, and 5  $\text{A/dm}^2$ .

Table 1. Composition of solutions for alloy electrodeposition.

$\text{ZnCl}_2$	$\text{NiCl}_2 \cdot 6\text{H}_2\text{O}$	KCl	$\text{H}_3\text{BO}_3$	$\text{CH}_3\text{COONa}$	560 BASE	560 Additive H	560 Brightener
					Performa Coventya (mL/L)		
52 g/L	81 g/L	250 g/L	20 g/L	35 g/L	75	50	1

Table 2: Composition of solutions and conditions for the subsequent trivalent chromium conversion treatment on the electroplated Zn-Ni alloy.

$[\text{Cr}^{3+}]$	$\text{NH}_4\text{HF}_2$	Temperature	pH	time
5 g/L	3 g/L	25 ( $^\circ\text{C}$ )	2	30 s

The subsequent trivalent chromium conversion treatment on the electroplated Zn-Ni alloy was performed in solution bath with composition of solutions and conditions shown in Table 2.

## 2.2. Analysis

The polarization curves were examined with sweep rate of 2 mV/sin 3.5 % NaCl solution by using biologic VSP-300 connected with a three electrode cell, including saturated calomel electrode (SCE), platinum counter electrode, and working electrode as subsequent trivalent chromium conversion treatment on the electroplated Zn-Ni alloy obtained by varying current density and time.

Scanning electron microscopy (SEM) images were taken by HITACHI S-4800 microscope. The phase structure of coatings was studied using X-ray diffraction (XRD). The electroplated Zn-Ni alloy composition was determined by X-ray fluorescence (XRF) spectrometer XRF 5006 – HQ02 and software XRF-FP Version 4.3.

The salt spray testing of these treated samples was performed on Q-FOG CCT-600 according to the standard JIS H8502. The samples were exposed to 5 % NaCl fog in a salt spray chamber at 35 °C. The coverage of the sample surfaces by the white and red corrosion products was recorded.

## 3. RESULTS AND DISCUSSION

### 3.1. Effects of current density on phase composition layer of zinc nickel alloy plating

According to the publications [9-11] there are 5 known phases for zinc-nickel alloys, including  $\eta$ - (1 % Ni),  $\alpha$  and  $\beta$ - (30 % Ni, known as the nickel rich phase),  $\delta$ - ( $\text{Ni}_3\text{Zn}_{22}$ ) and  $\gamma$ - ( $\text{Ni}_5\text{Zn}_{21}$ ) (known as the zinc rich phase).

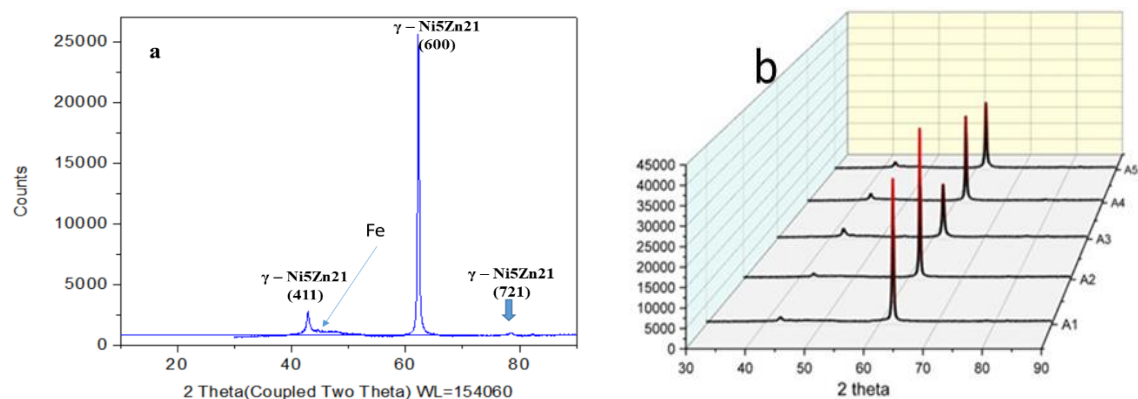


Figure 1. X-ray diffractogram of electroplated Zn-Ni alloy plating (A1: 1 A/dm<sup>2</sup>, A2: 2 A/dm<sup>2</sup>, A3: 3 A/dm<sup>2</sup>, A4: 4 A/dm<sup>2</sup>, A5: 5 A/dm<sup>2</sup>).

XRD diffractogram of electroplated Zn-Ni alloy in Fig. 1a shows the appearance of only  $\gamma$  phase. The zinc-nickel alloy of interest has a body centered cubic (bcc) lattice structure and has a chemical formula of  $\text{Ni}_5\text{Zn}_{21}$ . It confirms that the presence of  $\gamma$  phase Zn-Ni preferentially deposited onto the substrate. The observed 3 diffracted planes of (411), (600), and (721) reflect the presence of  $\gamma$  phase in the pattern (per pdf #00-006-0653 JCPDS Database). The deposit

exhibits the best corrosion protection when pure  $\gamma$  phase is only present [11]. The sole presence of  $\gamma$  phase in the electroplated alloy assures it ideal for corrosion protection.

Phase  $\gamma$  (the plane of  $\text{Ni}_5\text{Zn}_{21}$  (600)) is prioritized and can be influenced by the components for creating shine, 560 BASE, 560 Additive H, and 560 Brightener used in the KCl solution.

### 3.2. Effects of current density on the composition layer of zinc nickel alloy plating and efficiency

XRF spectrum of electroplated Zn-Ni alloy plating in Fig. 2 and Ni- content of Zn-Ni coatings prepared at different current densities in Fig. 3 show that the content of Zn-Ni coatings prepared in the KCl solution with 560 BASE, 560 Additive H, and 560 Brightener is about 12 ÷ 15 %. The Ni contents exhibited declining trend by increasing the current density.

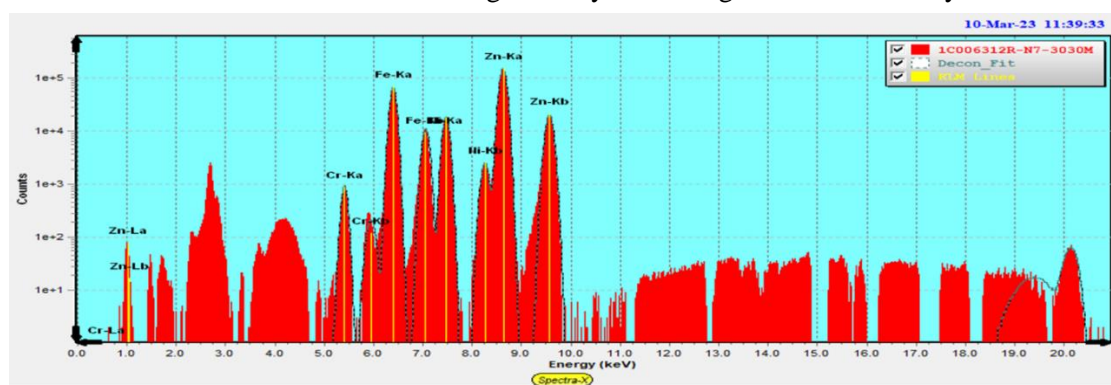


Figure 2. XRF spectrum of Zn-Ni alloy coatings.

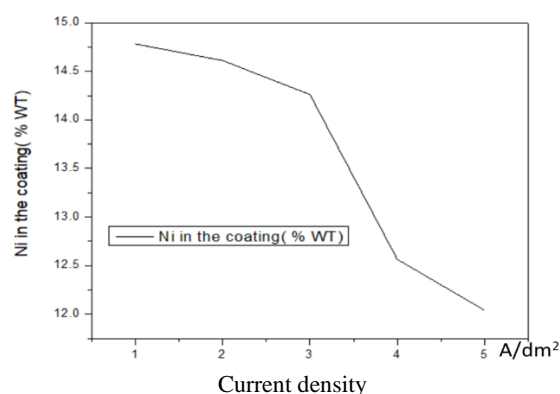


Figure 3. Ni- content of Zn-Ni coatings prepared at different current densities.

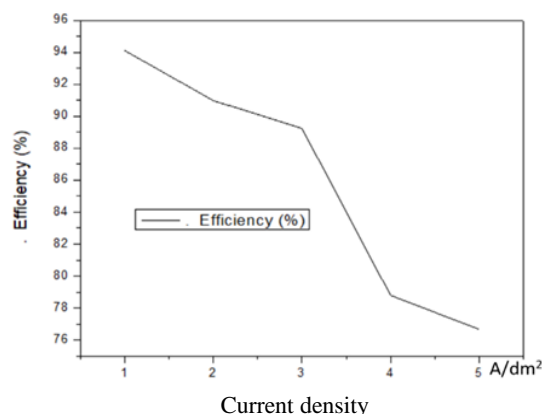
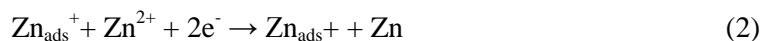


Figure 4. Efficiency at different current densities.

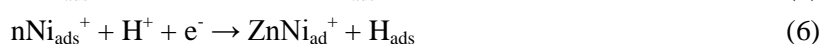
In the literatures [12-14], it is suggested that the preferential deposition of nickel is attributed to a mixed intermediate  $\text{ZnNi}_{\text{ad}}^+$  which catalyzes the reduction of nickel ion. The preferential deposition of zinc is attributed to the intermediate  $\text{Zn}_{\text{ads}}^+$  which play a catalytic role on the deposition of zinc rich coatings. In order to account for the above experimental results, the kinetics are applied.

Surface of the electrode is covered by intermediate  $\text{Zn}_{\text{ads}}^+$  (reaction (1)), which catalyzes the reduction of zinc ion (reaction (1)). Beside the primary reactions (1) and (2), also reaction (3)

probably takes place on the electrode surface with a low rate, so a small quantity of nickel can be found in the coating.



With the reduction of deposition current densities, the reaction (2) is partially blocked because of the formation of a mixed intermediate  $\text{ZnNi}_{\text{ad}}^+$  (reaction (4)) which catalyzes the nickel deposition (reaction (5)) and hydrogen evolution (reactions (6) and (7)) at the electrode surface. Subsequently, the nickel rich layer forms.



According to the publication [15], higher current densities provide more reductive circumstance and consequently more activation energy for deposition. This is more beneficial for deposition of the species that are dominantly controlled by kinetics rather than that controlled by diffusion. Due to higher concentration,  $\text{Zn}^{2+}$  ion deposition is more affected by kinetic parameters (e.g. current density) in comparison to that of  $\text{Ni}^{2+}$  ions. Therefore, with increasing the current density the contribution of  $\text{Zn}^{2+}$  ions in electron transfer is enhanced and its content in the deposits increases, which is equivalent to the reduction of the relative amount of Ni in the deposits.

It is acknowledged that as the Ni content is less than 15%, Zn-Ni alloys are sacrificial (active) to the steel substrate and in higher percentage the alloy would be passive. Also increasing in Ni content improves the corrosion resistance and the corrosion potential shifts to the positive direction [15].

Figure 4 indicates that plating efficiency tends to decrease by increasing the current density. It shows that the highest efficiency (94.1%) is gained at current density of 1 A/dm<sup>2</sup>, while the smallest efficiency (74.67%) is at current density of 5 A/dm<sup>2</sup>. This result is also consistent with glancing angle ( $2\Phi = 30-60^\circ$ ) on the XRD spectrum of electroplated Zn-Ni alloy coating with a peak at  $2\theta$  of  $45.5^\circ$  for Fe(0) with the greatest intensity corresponding to the plating layer with the smallest thickness. When increasing the current density, the process of hydrogen escape increases, causing an energy loss, which reduces efficiency.

### **3.3. Effects of current density on color and FESEM images of trivalent chromium passive film (TCP) on Zn-Ni alloy plating**

Images and color of TCP film on the Zn-Ni alloys deposited at different current densities are shown in Fig. 5.

As shown in Fig. 5, the TCP film on the Zn-Ni alloys deposited at current density of 1 A/dm<sup>2</sup> has the darkest rainbow color with characteristic blue color, while it is also in rainbow color at current density of 2 A/dm<sup>2</sup>, but the characteristic colors are blue and yellow-brown which are lighter in comparison with that at current density of 1 A/dm<sup>2</sup>. The color of passive films gradually fades with increasing current density.

In combination with section 3.2 on the Ni-content of Zn-Ni coatings prepared at different current densities, it is shown that, plating layers containing higher Ni content give the passive film with a darker color. At current density of 5 A/dm<sup>2</sup>, they have the lowest Ni content and the passive films are in the lightest color.

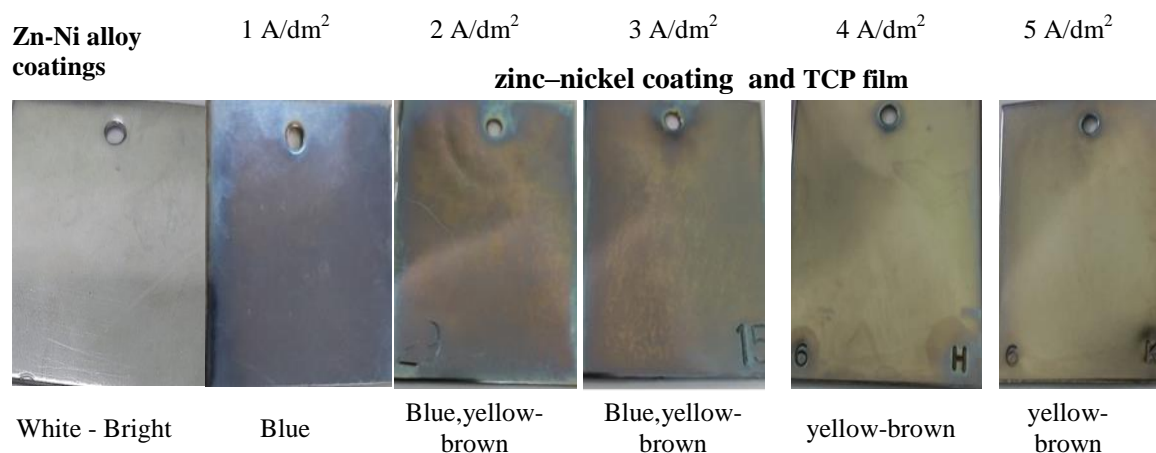


Figure 5. Images and color of TCP films on the Zn-Ni alloys deposited at different current densities.

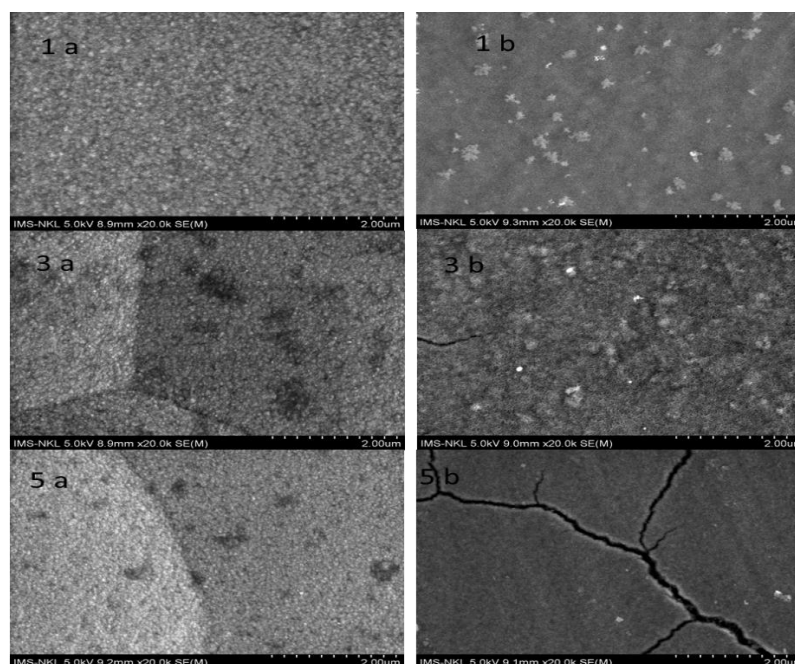


Figure 6. SEM images of electrodeposited Zn-Ni coating and TCP film on the Zn-Ni alloys deposited at different current densities.

SEM images of electrodeposited zinc–nickel coating are shown in Fig. 6 (1a, 3a, and 5a). SEM images of TCP on the Zn-Ni alloys deposited at different current densities are shown in Fig. 6 (1b, 3b, and 5b). Figure 6 shows that electrodeposited zinc–nickel coatings at current density of 1, 3, and 5 A/dm<sup>2</sup> in the KCl solution used 560 BASE, 560 Additive H, and 560 Brightener have fine plating particles with dimensions in the range of 0.01 ÷ 1 µm. These sizes

are significantly smaller than that in the publication [8], the dimensions of particle in Zn-Ni alloy plating in borate electrolytic alkaline solution are in the range of  $1 \div 3 \mu\text{m}$ .

As shown in Fig. 6 (1b, 3b, 5b), the TCP films on the Zn-Ni alloys deposited have a smooth surface morphology. There are cracks at current densities of 3 and 5  $\text{A}/\text{dm}^2$ .

### 3.4. Effects of current density on corrosion resistance of electrodeposited Zn-Ni coating and TCP film on the Zn-Ni alloy deposits

Polarization curves of the samples for electrodeposited zinc–nickel coating and TCP film on the Zn-Ni alloys deposited at different current densities are shown in Fig. 7.

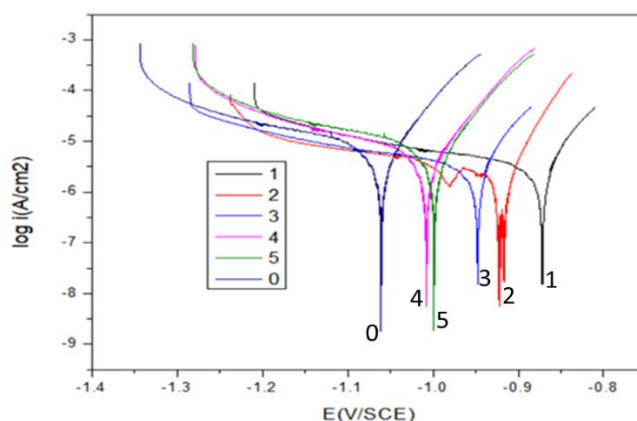


Figure 7. Polarization curves of the electrodeposited zinc–nickel coating and TCP film on the Zn-Ni alloys deposited at different current densities (notation sample as present in Table 3) .

Table 3. Potentiodynamic polarization data and time for white rust, red rust appearing.

Sample	$i(\text{A}/\text{dm}^2)$	% Ni	notation sample	$i_{\text{corr}} (\mu\text{A}/\text{cm}^2)$	$E_{\text{corr}}(\text{V}/\text{SCE})$	white rust(h)	Red rust(h)
Zn-Ni alloycoatings	1	14.71	0	6.866	1,069	24	600
TCP film on Zn-Ni alloy coatings	1	14.71	1	3.777	-0.8721	552	1200
	2	14.56	2	3.308	-0.9211	504	1128
	3	14.31	3	2.077	-0.9895	480	1128
	4	12.565	4	5.87	-1.0081	480	1080
	5	12.04	5	2.22	-0.9977	480	960

Potentiodynamic polarization data and time for white rust and red rust appearing in Table 3 show that: (i) the corrosion potential of the passive samples is more positive than that of the non-passive samples. This can be explained by the increase in Ni content on the surface due to the dissolution of Zn being greater than the dissolution of Ni upon passivation (Zn is more active than Ni); (ii) the corrosion rate ( $i_{\text{corr}}$ ) of the passive samples was significantly lower than that of



the non-passive Zn-Ni alloy sample. In passive samples, the corrosion rate is only half of non-passive samples. Thus, the effectiveness of the passive process can be clearly seen.

When comparing TCP films on the Zn-Ni alloys deposited at different current densities, with the reduction of deposition current densities, the Ni content in the coating increases, the corrosion potential shifts toward the positive, corrosion current density is reduced, and the corrosion resistance of the coating is improved.

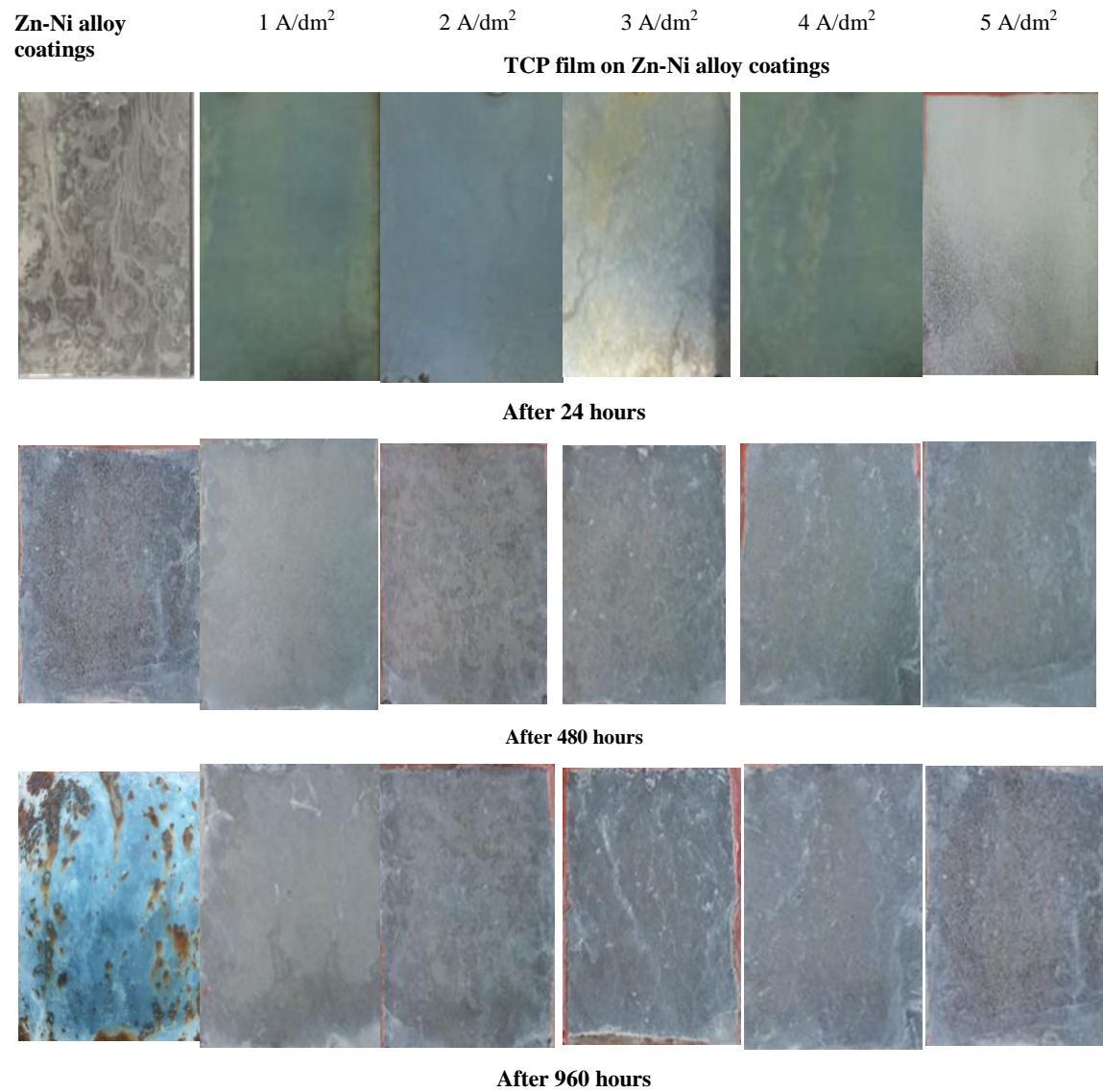


Figure 8. Surface appearance of prepared coatings before and after exposure to salt spray.

Figure 8 shows the surface of coatings before and after exposure to salt spray. As seen in Fig. 8, for non-passive samples (white samples), white rust appears within the first 24 hours, after 480 ÷ 552 hours of exposure to salt spray the surface of TCP films on the Zn-Ni alloys deposited has white rust. After 960 hours of exposure to salt spray, there are red rust on the surface of TCP films on the Zn-Ni alloys deposited at current density of 5 A/dm<sup>2</sup>, with the TCP



films on the Zn-Ni alloy deposited at current density of 1 A/dm<sup>2</sup> the time to have red rust is 1200 hours. The presence times of red rust on TCP films on the Zn-Ni alloys deposited at current density range of 1÷4 A/dm<sup>2</sup> are 1080 ÷ 1128 h. According to DIN EN ISO 19598:2017-04 standard, the corrosion resistance requirement of rainbow-colored zinc-nickel passive layers is that no white rust appears within 360 hours (according to ISO 9227) when suspended plating. All of TCP films on the Zn-Ni alloys deposited at different current densities meet DIN EN ISO 19598: 2017-04 standards.

#### 4. CONCLUSIONS

The obtained results indicated that the Ni content in Zn-Ni alloy electrodeposited coating is 12 – 15 %. The electrodeposited coating crystal is that of  $\gamma$  phase alloy which is ideal for corrosion protection. The zinc-nickel alloy of interest has a body centered cubic (bcc) lattice structure and has a chemical formula of Ni<sub>5</sub>Zn<sub>21</sub>. Plating efficiency tends to decrease by increasing the current density. Efficiency at current density of 1 A/dm<sup>2</sup> is the highest, 94.1 %. SEM images of electrodeposited zinc–nickel show fine plating particles with dimensions in the range of 0.01 ÷ 1  $\mu$ m.

The TCP film on the Zn-Ni alloys deposited is in rainbow color with characteristic blue, yellow-brown color. The color of passive films gradually fades with increasing current density. Plating layers containing higher Ni content give the passive film a darker color. The corrosion potential of the passive samples is more positive than that of the non-passive samples. The corrosion rate ( $i_{\text{corr}}$ ) of the passive samples was significantly lower than that of the non-passive Zn-Ni alloy sample. For non-passive samples (white samples), white rust appears within the first 24 hours; after 480 ÷ 552 hours of exposure to salt spray, the surface of TCP films on the Zn-Ni alloys deposited has white rust. After 960 ÷ 1200 hours of exposure to salt spray, there are red rust on the surface of TCP films on the Zn-Ni alloys deposited at current density 1 ÷ 5 A/dm<sup>2</sup>. All of TCP films on the Zn-Ni alloys deposited at different current densities meet DIN EN ISO 19598: 2017-04 standards.

**Acknowledgment.** This work was supported by the Key Science and Technology Project of Vietnam Academy of Science and Technology (Grant No: TĐVLTT.05/21-23).

**Data Availability.** The figures and table data used to support the findings of this study are included within the article.

**Author statement:** Le Ba Thang: Writing - Review & Editing, Supervision, Funding acquisition, Project administration; Truong Thi Nam: Conceptualization, Writing - Original Draft, Formal analysis, Visualization; Le Duc Bao: Validation, Investigation; Nguyen Thi Thanh Huong: Investigation; Uong Van Vy: Investigation; Le Thao Ly: Investigation.

**Conflicts of Interest.** The authors declare that there are no conflicts of interest regarding the publication of this paper.

#### REFERENCES

1. Foster K., Claypool J., Fahrenholtz W. G., O'Keefe M., Nahlawi T., Almodovar F. - Characterization of cobalt containing and cobalt-free trivalent chromium passivations on  $\gamma$ -ZnNi coated steel substrates, *Thin Solid Films* **735** (2021) 138894.

2. Lotfi N., Aliofkhazraei M., Rahmani H. & Barati Darband Gh. - Zinc – Nickel alloy electrodeposition: Characterization, Properties, Multilayers and Composites, *Protection of Metals and Physical Chemistry of Surfaces* **54** (2018) 1102-1140.
3. Bhat R. S., Shetty S. M., and Anil Kumar N. V. - Electroplating of Zn-Ni Alloy Coating on Mild Steel and Its Electrochemical Studies, *Journal of Materials Engineering and Performance* **30** (2021) 8188-8195.
4. Lotfia N., Aliofkhazraeia M., Rahman H., and Barati Darbanda Gh. - Zinc–Nickel Alloy Electrodeposition: Characterization, Properties, Multilayers and Composites, *Protection of Metals and Physical Chemistry of Surfaces* © Pleiades Publishing, Ltd., 2018.
5. Zaki N. - Trivalent chrome conversion coating for zinc and zinc alloys, *Metal Finishing* **105** (10) (2007) 425- 435.
6. Kozaderov O., Światowska J., Dragoe D., Burliaev D., Volovitch P. - Effect of Cr(III) passivation layer on surface modifications of zinc-nickel coatings in chloride solutions, *Journal of Solid State Electrochemistry* **25** (4) (2021) 1161-1173.
7. Conrad H. A., McGuire M. R., Zhou T., Coskun M. I., Golden T. D. - Improved corrosion resistant properties of electrochemically deposited zinc-nickel alloys utilizing a borate electrolytic alkaline solution, *Surface & Coatings Technology* **272** (2015) 50-57.
8. Sheu H. H., Lee H. B., Jian S.Y., Hsu C.Y., Lee C.Y. - Investigation on the corrosion resistance of trivalent chromium conversion passivate on electroplated Zn –Ni alloy, *Surface & Coatings Technology* **305** (2016) 241-248.
9. Wykpis K., Popczyk M., Niedbala J., Budniok A., Lagiewka E. - Influence of the Current Density of Deposition on the Properties of Zn-Ni Coatings, *Materials Science* **47** (6) (2012) 838-847.
10. Selvaraju V. and Thangaraj V. - Influence of  $\gamma$ -phase on corrosion resistance of Zn–Ni alloy electrodeposition from acetate electrolytic bath, *Material Research Express* **5** (2018) 056502.
11. Michael M.S. and Radhakrishna S. - Effect of heat treatment on the corrosion performance of electrodeposited zinc alloy coatings, *Anti-Corrosion Methods and Materials* **45** (1998) 113-119.
12. Fabri Miranda F.J., Barcia O.E., Mattos O.R. - Electrodeposition of Zn–Ni alloys in sulfate electrolytes. I. Experimental, *Journal of the Electrochemical Society* **144** (1997) 3441-3448.
13. Chassaing E., Wiart R. - Electrocrystallization mechanism of Zn–Ni alloys in chloride electrolytes. *Electrochimica Acta* **37** (1992) 545-553.
14. Fabri Miranda F. J., Barcia O.E., Matto O.R. s - Electrodeposition of Zn–Ni alloys in sulfate electrolytes. II. Reaction modeling, *Journal of the Electrochemical Society* **144** (1997) 3449-3457.
15. Bahadormanesh B., Ghorbani M. - Electrodeposition of nanocrystalline Zn/Ni multilayer coatings from single bath: Influences of deposition current densities and number of layers on characteristics of deposits, *Applied Surface Science* **404** (2017) 101-109.